HOKKAIDO UNIVERSITY

Title	Effects of metal cations on mild steel corrosion in 10 mM Cl- aqueous solution
Author(s)	Islam, Md. Saiful; Otani, Kyohei; Sakairi, Masatoshi
Citation	Corrosion Science, 131, 17-27 https://doi.org/10.1016/j.corsci.2017.11.015
Issue Date	2018-02
Doc URL	https://hdl.handle.net/2115/76657
Rights	© 2018. This manuscript version is made available under the CC-BY-NC-ND 4.0 license http://creativecommons.org/licenses/by-nc-nd/4.0/
Rights(URL)	https://creativecommons.org/licenses/by-nc-nd/4.0/
Type	journal article
File Information	Saiful_Accepted_Manuscript.pdf

Hokkaido University Collection of Scholarly and Academic Papers : HUSCAP

Title

Effects of metal cations on mild steel corrosion in 10 mM Cl^- aqueous solution

Author Names

Md. Saiful ISLAM[1)], Kyohei OTANI[1)], Masatoshi SAKAIRI[2)]

Affiliations

1) Graduate School of Engineering, Hokkaido University, Kita-13, Nishi-8, Kita-ku, Sapporo, Hokkaido 060-8628, Japan.
2) Faculty of Engineering, Hokkaido University, Kita-13, Nishi-8, Kita-ku, Sapporo, Hokkaido 060-8628, Japan.

Abstract

The influences of metal cations on the corrosion of mild steel in 10 mM Cl^- aqueous solutions were investigated by electrochemical techniques and immersion tests. Immersion tests and electrochemical impedance spectroscopy (EIS) results showed that Zn^{2+} has a significant effect on corrosion inhibition. Surface morphological inspection also showed the smooth surface of specimen immersed in Zn^{2+} containing solution. Analysis of X-ray photoelectron spectroscopy showed that Zn^{2+} was incorporated in the oxide films by making a strong bond. It is supposed that Zn^{2+} forms a very effective shielding film which can inhibit the electrochemical reactions, and consequently lowers the corrosion rate.

Keywords

Mild steel; EIS; XPS; SEM; Passive films

1. Introduction

The stability of a metal when exposed to the environment depends on a multitude of factors that may vary greatly with the concentration of Cl^- and SO_4^{2-} of that environment. Mild steel is very popular and widely used metallic materials, and the corrosion of this steel is a serious problem in water supply, storage tanks and circulating water pipes etc., and the corrosion behavior have been studied by many researchers [1-3]. The corrosion rate of mild steel can be accelerated by the presence of the compound that may contains Cl^- and SO_4^{2-} [4-6]. Large amount of chlorine compounds (Cl_2, NaOCl, $Ca(OCl)_2$ etc.) are used as disinfectants in the waste water treatment and bleach for both domestic and industrial purposes. These compounds are also widely used to disinfect drinking water and swimming pool water, and to control bacteria and odors in the food industry [7-9]. Enormous amount of chlorine compounds is also used in the laundry to bleach and wash the cloths. Chlorine compounds are listed as a known poison and it has an adverse effect on corrosion of the pipe line of water circulation system and other metallic equipment that exposed in that environment, and these compounds are dissociated into Cl^- and OCl^- in the aqueous solution as following reactions.

$$Cl_2 + H_2O \rightarrow H^+ + Cl^- + HOCl \quad (1)$$

$$NaOCl + H_2O \rightarrow NaOH + H^+ + OCl^- \quad (2)$$

$$Ca(OCl)_2 + H_2O \rightarrow Ca(OH)_2 + H^+ + OCl^- \quad (3)$$

The oxide layer (passive film) of the steel is generally destroyed by the penetration of Cl^- in aqueous solution [4, 10-13]. Fig. 1 (a) and (b) shows the penetration and film thinning mechanism of Cl^- into the oxide films [14-17]. After destruction of the passive films, the corrosion process starts with a coupled of electrochemical reactions [1, 2, 18]. Fig. 1 (c) shows the anodic reaction of metal dissolution (reaction (4)) and cathodic reaction of oxygen reduction (reaction (5)).

$$Fe\ (s) \rightarrow Fe^{2+}\ (aq) + 2e^- \quad (4)$$

$$1/2O_2 + H_2O + 2e^- \rightarrow 2OH^- \quad (5)$$

Otani et al. [18, 19], Kato [20] and Takasaki [21] investigated the corrosion behavior of mild steel by emphasizing the effects of metal cations in model fresh water, and they found that Zn^{2+} and Al^{3+} have ability to inhibit the corrosion. Mahdavian et al. [22] investigated the corrosion inhibition of mild steel by some zinc complexes in sodium chloride solution. Prabhu et al. [23] investigated the corrosion behavior of metal surface treated with a new organic chelating inhibitor in acid solution. Jin-xia Xu et al. [24] investigated the steel corrosion in saturated calcium hydroxide solution with metal oxides and nitrates. For this reason, the effect of metal cations on the corrosion of mild steel should be considered in the Cl^- containing aqueous solution. The effect of metal cations on corrosion of mild steel in 10 mM Cl^- aqueous solution is not fully understood. Therefore, it is needed to clarify the effect of metal cations on corrosion behavior of mild steel in the solution that contains 10 mM Cl^- at an equal level of pH.

Incorporation of the metal cations in the passive films would be significant to clarify the influence of metal cations on the corrosion of mild steel in the 10 mM Cl^- aqueous solution. According to the Lewis concept regarding acid and bases, cations and anions act as acids and bases, respectively [25]. Further, acids and bases are categorized into 'hard' and 'soft' [26]. According to the hard and soft acid and base (HSAB) concept, soft acids react and form strong bonds with soft bases, whereas hard acids react and form strong bonds with hard bases. The metal cation hardness is based on the HSAB concept. The hardness of metal cations, X, is expressed as follows [18, 27, 28]:

$$X = [X^0_M + (\Sigma I_n)^{1/2}]^2 / 10 \quad (6)$$

Where X^0_M is the electronegativity of the metal atom, and I_n (eV) is the ionization potential from the neutral metal atom to the given oxidized state, n. Hard acids and hard bases can form stable bonds. Hydroxyl groups, which are categorized as hard bases, are located on the outermost layer of oxide film of mild steel and metal cations with large X, which are

categorized as hard acids therefore easily bond with hydroxyl groups on the mild steel. For this reason, the value of *X* indicates the tendency of formation of chemical bond between metal cations in the solution and hydroxyl groups on the mild steel surface. Therefore, HSAB concept is very useful for understanding the incorporation of metal cations in the oxide films [29]. Based on the HSAB concept, hardness of metal cation, *X* was introduced to explain the corrosion behavior of metals in fresh water [27]. However, *X* is not suitable corrosion indicator regarding corrosion of metals in fresh water [18]. It is still unknown the possibility of *X* as an indicator for corrosion of metals in the 10 mM Cl^- aqueous solution. The mechanism of corrosion inhibition of metal cations is also unknown. By considering the corrosion rate of mild steel that depends on the metal cations [18, 19], Cl^- concentration, pH [30, 31] and dissolved oxygen, the present research purpose is to find out the effects of metal cations on corrosion of mild steel, and the mechanism of corrosion inhibition in 10 mM Cl^- aqueous solution at an equal level of pH.

In this experiment, comparative conditions were used to study the influence of metal cations on corrosion of mild steel in 10 mM Cl^- aqueous solution. The fluctuations of environmental factors were controlled initially to obtain the effective influence of metal cations on corrosion. The influence of metal cations on corrosion of mild steel in the mentioned environment were investigated by electrochemical impedance spectroscopy (EIS), immersion tests, surface observation and analysis with scanning electron microscope (SEM), Energy dispersive X-ray spectroscope (EDS) and X-ray photoelectron spectroscope (XPS).

2. Experimental

2.1 Specimens

Mild steel sheets (7 × 7 mm in size and 0.7 mm in thickness) were used as specimens. The chemical composition of the mild steel is shown in the Table 1. The methods used to prepare

specimens for immersion tests and electrochemical measurements are shown in Fig. 2. To make an electrical contact, a wire was connected with each specimen to perform the electrochemical measurements. All the specimens were molded in epoxy resin (Struers Ltd., EpoFix Resin). The exposed surface of each molded specimen was grounded (Marumoto Struers S5629, LaboForce-3) with SiC abrasive papers from #400 to #4000 grit size, then finally polished by colloidal silica. Before the immersion tests, the specimens were taken out from the epoxy resin. All the specimens were ultrasonically cleaned (SIBATA ultrasonic cleaner, SU-2T) in ethanol and then in highly purified water. The specimens were kept in a desiccator to avoid any type of contamination and humidity.

2.2 Solutions

Five different salt solutions, 10 mM NaCl (Na_{sol}), 0.1 mM $MgCl_2$ (Mg_{sol}), 0.1 mM $ZnCl_2$ (Zn_{sol}), 0.1 mM $AlCl_3$ (Al_{sol}), and 0.1 mM $ZrOCl_2$ (Zr_{sol}) were used as test solutions. The Cl^- concentration was adjusted to 10 mM by NaCl. In this study, Na_{sol} was considered as a standard solution. Water used in this study was highly purified that was distilled two times and then further purified by water purifier (MILIPORE, Simplicity UV). All chemicals used in this study were special analytical grade and obtained from Kanto Chemical Co. Ltd.

Electrochemical reactions are mostly depended on the pH of the aqueous solution [30, 31]. The pH of used solutions was controlled between 5.5 and 6.0 by 0.1 M NaOH (Table 2). The pH measurement of the solutions before and after immersion tests were carried out using the pH meter (Eutech Instruments Pte. Ltd., Cyber-Scan 6000).

2.3 Immersion tests

Specimens were immersed in the solutions for 259.2 ks (3 d) at 25°C. The test performing bottles were open to the air during immersion tests. The mass of the specimens was measured using a micro-balance (METTLER TOLEDO MX5, Pro FACT) before and after immersion tests, and the corrosion rates were calculated from the mass variation using the equation (7).

$$\text{Corrosion rate } (\mu m/y) = \frac{(M_1 - M_2)}{D \times S \times t} \times 3650 \quad (7)$$

Where M_1 is mass before immersion (mg), M_2 is mass after immersion (mg), D is density of specimen (g/cm^3), S is surface area of specimen (cm^2) and t is immersion time (d).

2.4 Electrochemical tests

All the electrochemical measurements were carried out in a three-electrode system using a potentiostat (Pocketstat, IVIUM TECHNOLOGIES). Open-circuit potential (OCP) was measured for 1 h at 25°C and the potentiodynamic measurements were carried out in the cathodic and anodic direction with a scan rate of 1 mV/s. The cathodic and anodic scan was started separately to obtain the individual electrochemical properties of mild steel immersed in the corresponding solutions with metal cation. A platinum plate of 4 cm^2 and an Ag/AgCl electrode (SSE) immersed in a saturated KCl solution were used as counter and reference electrodes, respectively. The exposed surface area of working electrode in the solution was 49 mm^2. EIS measurements were carried out in the frequency range from 10 kHz to 1 mHz, and a modulation amplitude of 10 mV. Reproducible data were acquired in all electrochemical measurements.

2.5 Surface observations and analysis

Surface morphology is the important criteria which reflects the corrosion behavior of the mild steel regarding the solution. Surface observation of specimen after immersion were carried out to clarify the variance of the specified corrosion behavior of mild steel in the different solutions of metal cation. Before and after the immersion tests, the surfaces of the specimens were observed by a digital camera (Nikon D80-DSLR), optical microscope (WRAYMER-G500) and Scanning Electron Microscope (SEM) using secondary electrons imaging (SEM, JEOL Ltd., JSL6510-LA). For SEM observation, the acceleration voltage of the electron beam was set at 10 kV in order to be sensitive to the morphology of the surface. EDS analysis was carried out to analyze the surface composition of the specimen after

immersion tests.

Surface analysis was carried out to clarify the situation of specimen surface after immersion in the solutions with different metal cation. The center area of the specimens after immersion was analyzed by X-ray Photoelectron Spectroscope (XPS, JEOL Ltd., JPS-9200) using a monochrome Al Kα X-ray source. Before the analysis, the immersed specimens were cleaned ultrasonically by ethanol and then in highly purified water. After cleaned, specimens were kept in a desiccator to avoid humidity and any type of contamination. The diameter of specimen analyzed by the XPS was 3 mm.

3. Results

3.1 Immersion tests

Fig. 3 (a) shows the appearance of specimens at the starting of immersion and 3 (b) shows the specimens after immersion in Na_{sol}, Mg_{sol}, Zn_{sol}, Al_{sol} and Zr_{sol} during 259.2 ks (3 d) at 25°C. In Fig. 3 (b), there are many brown color corrosion products are observed on the specimen surface in the case of Na_{sol}, and Mg_{sol}. The amounts of corrosion products in Zn_{sol}, Al_{sol}, and Zr_{sol} are decreased compared with Na_{sol} and Mg_{sol}. Fig. 3 (c) shows the surface images of specimens after immersion in the solutions before (upper row) and after (bottom row) ultrasonic cleaning. Brown color corrosion products were deposited on the specimen surface that were observed before ultrasonic cleaning, and the amount was varied depending on the solutions. Less amount of brown color corrosion products is observed in the case of Zn_{sol} as compared to the other solutions. The corrosion rates were calculated from the mass loss after immersion for 259.2 ks (3 d) in the different solutions. The density of specimen, 7.874 g/cm^3 was used to calculate the corrosion rates [32]. Fig. 4 shows the corrosion rate as a function of *X*. The corrosion rate is gradually decreased with increasing the value of *X* up to 5, and over 5, the corrosion rate is not decreased gradually. The correlation coefficient is -0.42 indicating that

corrosion rate is not clearly related with *X*. However, the results of immersion corrosion tests indicate that Zn_{sol} has the better corrosion inhibition effect on mild steel in high concentration of Cl^- containing aqueous solution.

The pH of the test solutions before and after immersion for 259.2 ks (3d) are shown in Table 2. Initial pH (pH_{int}) of Al_{sol} and Zr_{sol} showed low value than other solutions of metal cation and it were adjusted (pH_{adj}) to 5.7 and 5.8. Average pH of the test solutions is around 5.8. The pH was slightly increased after immersion (pH_{corr}) in all solutions of metal cations for 259.2 ks due to the formation of OH^- at the metal surface [18, 33].

3.2 Electrochemical tests

3.2.1 Open-circuit potential (OCP) and potentiodynamic polarization

The open circuit potentials of mild steel measured in the solution of metal cations rapidly reach a stable value after around 3000 s of immersion (Fig. 5 (a)). All the measured values are confined in a reduced range of potentials between -0.22 V and -0.45 V. Only slight difference can be noticed in the case of Mg_{sol}, Zn_{sol}, Al_{sol} and Zr_{sol} as compared to Na_{sol}, and Na_{sol} induces the most negative open-circuit potential and Zn_{sol} the most positive one. Open-circuit potentials at 1 s and at 3000 s as a function of *X* are shown in Fig. 5 (b). The metal cations which have large *X* show no significant difference. However, Zn_{sol} shows higher average potential than Na_{sol}, and Na_{sol} shows the lowest average potential at 3000 s as compared to the other solutions with metal cations.

Fig. 6 (a) shows the cathodic polarization curves and Fig. 6 (b) shows the anodic polarization curves. From the Figs. 6 (a) and (b) (indicated by arrow), it is found that Zn_{sol} shows lower current density as compared to the Na_{sol} and Na_{sol} shows the highest current density among used solutions both in cathodic and anodic polarization curves. For the other solutions of metal cation, there is no significant influences of cathodic and anodic reactions as well.

3.2.2 Electrochemical Impedance Spectroscopy (EIS)

EIS measurements were carried out to elucidate the initial corrosion behavior of the mild steel and the effect of metal cations on the properties of the protective layer. Fig. 7 shows the Bode diagram of (a) Impedance plots, (b) phase shift plots and (c) Nyquist plots of the mild steel in the solutions after immersion for 1 h, and impedance spectra depend on the kinds of metal cations. There was no rust formed during EIS measurements. The fitted lines calculated by Randle's equivalent circuit model [34-36] are also shown in Fig. 7, and the equivalent circuit model is shown in Fig. 7 (d). All the spectra can be well described by equivalent circuit. This model consists of solution resistance (R_{sol}), charge-transfer resistance (R_{ct}), and constant phase element (CPE), Q. The impedance can be expressed in terms of R_{sol}, R_{ct} and CPE parameters n and Q by equation (8) [37-40].

$$Z = \mathrm{R_{sol}} + \frac{\mathrm{R_{ct}}}{1+ (j\omega)^n \, \mathrm{QR_{ct}}} \tag{8}$$

Where $\omega = 2\pi f$ and f is the frequency in units of Hz. The value of CPE parameter, n varies from 0 to 1. When n = 1, the CPE behaves as a pure capacitor, and when n = 0, the CPE behaves as a pure resistor. The CPE parameters are calculated by using the equation (8). The simulated values of CPE parameters are shown in the table 3.

The magnitude of impedance at low frequencies in Bode diagram implies the corrosion resistance of mild steel in the solution. Among five experimental solutions, Zn_{sol} shows the larger impedance at low frequency (Fig. 7 (a)). Higher phase shift is observed for Zn_{sol} (Fig. 7 (b)), and magnitude of each Nyquist plots are different depending on the solutions (Fig. 7 (c)). Larger magnitude of Nyquist plot is observed in the case of Zn_{sol} among other solutions.

The (a) R_{sol}, (b) R_{ct}, and (c) Q as a function of X are shown in Fig. 8. The R_{sol} are not significantly changed with X (Fig. 8 (a)). Higher R_{ct} is observed in the case of Zn_{sol} (Fig. 8 (b)) than other solutions, and there are no significant influences for the other solutions. High R_{ct} means that the mild steel has high corrosion resistance in the solution. This is supposed that

Zn_{sol} exposes the high corrosion resistance (R_{ct}) than other solutions. The value of Q is decreasing with increasing the value of *X* up to 5 and then the Q is again increasing with increasing the value of *X* (Fig. 8 (c)). Zn_{sol} shows the lowest value of Q than other solutions of metal cation (Table 3). Q represents the structure of solution/metal interface and the area of defects in the protective film on the surface [19, 22]. Otani et. al [19] reported that the decrease in Q indicates that Zn^{2+} can decrease the defect in the protective film on the mild steel. Therefore, this result indicates that Zn_{sol} has relatively perfect oxide film and narrow metal/solution interface area than other solutions.

The results of EIS and immersion tests showed that the corrosion rate of the mild steel decreases with increasing the value of *X* up to 5. In addition, the correlation coefficients of R_{sol} vs *X*, R_{ct} vs *X*, and Q vs *X* are 0.51, 0.15 and -0.01 respectively (Fig. 8 (a), (b) and (c)), and these values are too small to regard corrosion rate with hardness of metal cations, *X*. Therefore, the hardness of metal cations, *X*, is not suitable as a corrosion indicator of mild steel in 10 mM Cl^- aqueous solution. The results obtained from EIS and immersion tests, suggest that Zn_{sol} has the high corrosion resistance over other metal cations used in this study in 10 mM Cl^- aqueous solution.

3.3 Surface observations and analysis

The results of immersion corrosion tests showed that the corrosion rates of the specimens after immersion for 259.2 ks (3 d) is different in each solution. The changes in the appearance of specimen surfaces were observed to clarify the situation. Specimen surface was first observed by optical microscope, and grain boundaries were observed. To be more clear about surface changes, observations were carried out by SEM. Fig. 9 shows the surface SEM images of specimen and quite different surface morphologies are observed for the different solutions. SEM images depict the clear grain boundaries that is observed in the case of Na_{sol}, Mg_{sol}, Al_{sol} and Zr_{sol}. Pits and grain boundaries is observed in the case of Na_{sol}. A few numbers of pits are

also observed for Mg_{sol}, Al_{sol} and Zr_{sol}, and some corrosion products are deposited on the surface in the case of Zn_{sol}. Zn^{2+} may form less soluble salts and tend to precipitate in a form of hydroxide, oxide, or hydroxy salts. Severe corrosion is observed for Na_{sol} as compared to the other solutions. The results suggest that corrosion may affected with corrosion inhibiting effect of the metal cation and Zn^{2+} has the better corrosion inhibition effect on mild steel in the 10 mM Cl^- aqueous solution. An EDS analysis result is shown in Fig. 10. Left side of Fig. 10 shows the SEM image of EDS analysis area, and right side shows the EDS analysis result, and Zn is found on the mild steel surface after immersion in the solution.

The results of the immersion corrosion tests and electrochemical measurements suggest that the protectiveness of passive film may be affected by the metal cations in the solution. For better understanding the influence of metal cations and also the incorporation of metal cations on the surface film structure, the specimen surfaces after the immersion tests were investigated by XPS. Fig. 11 shows the XPS wide spectra of mild steel surface after immersion in the solution with metal cations. This figure clearly shows the peak of Zn2p1/2 and Zn2p3/2 after immersion in the Zn_{sol}. Fig. 12 (a) shows the XPS narrow spectra of Na 1s and Fig. 12 (b) shows the Mg 1s, Zn 2p3/2, Al 2p3/2 and Zr 3d5/2 spectra in each solution. XPS analysis results show that there is no peak of Na 1s on the specimen after immersion in all solution suggesting that Na^+ cannot form any compound on the mild steel in the solution (Fig. 12 (a)). Clear peak is observed (Fig 12 (b)) in the case of Zn^{2+} among all experimental metal cations meaning that only Zn^{2+} remains on the mild steel after immersion in the solution. Zn^{2+} may precipitates as oxides or hydroxides [18, 19] and make a chemical bond with the oxide film of mild steel in 10 mM Cl^- aqueous solution and forms a metal cation layer which inhibits the anodic and cathodic reactions, and protects the dissolution of metal [18, 19]. These results correspond with other tests like as immersion tests and electrochemical tests.

4. Discussions

According to the results in this study, the corrosion properties of mild steel significantly affected by metal cations in the solution. Electrochemical measurements showed that the decrease of corrosion rate of mild steel due to an inhibitory effect of both the anodic reaction of iron oxidation and the cathodic reaction of oxygen reduction. This inhibitory effect might be the consequences of metal cation that was incorporated on the oxide films of the metal surface and suppress the corrosion rate.

The structure of passive films formed on mild steels in neutral solution has been reported by many researchers by electron diffraction, and the passive films consist of Fe_3O_4 and γ-Fe_2O_3 in neutral solutions [41-44]. The possible corrosion mechanism of metal cations with the passive film of mild steel in the 10 mM Cl^- aqueous solution is shown in Fig. 13. Metal cations (M^{n+} = Na^+, Mg^{2+}, Al^{3+}, and Zr^{4+}) are not able to make (Fig.13 (a)) any compound (precipitate) or unable to make any bond with the oxide film of mild steel (Fig.13 (b)). From the Pourbaix diagram, it is known that Mg^{2+} ([Mg^{2+} = 0.1mM]) and Zr^{4+} ([Zr^{4+} = 0.1mM]) cannot precipitate as oxides or hydroxides at pH lower than 8 [45]. After immersion, the pH of the solution was about 6.5 (Table 2). Therefore, Mg^{2+} and Zr^{4+} are not able to precipitate on the mild steel in this pH. Al^{3+} ([Al^{3+} = 0.1mM]) is able to form oxides or hydroxides on mild steel at pH lower than 6 [45]. However, the oxides or hydroxides are not stable [45, 46]. Then Cl^- can arrive on the metal surface through destroying the oxide films and initiate the electrochemical reactions. Consequently, Al_{sol} shows higher corrosion rate than Zn_{sol} (Fig. 4) in this experiment due to the instability of the oxides or hydroxides that are formed on mild steel [45, 46].

The possible corrosion mechanism of Zn^{2+} would be different from other metal cations (M^{n+} = Na^+, Mg^{2+}, Al^{3+}, and Zr^{4+}). EDS and XPS analysis results show the clear evidence that Zn^{2+} remains on the mild steel after immersion in the solution among metal cations used in this study. It is expected that Zn^{2+} reacts with the OH^- (reaction (5)) to form hydroxides (reaction

(9)) in the cathodic area due to locally high pH near the surface [33, 45, 47]. From the Pourbaix diagram, it is also known that Zn^{2+} ([Zn^{2+} = 0.1mM]) can precipitate as hydroxides on the mild steel at pH around 6 [45].

$$Zn^{2+} + 2OH^- \rightarrow Zn(OH)_2 \quad (9)$$

The mechanism of corrosion inhibition is as follows:

The produced hydroxides can possibly bind in a chemical bond with the outermost layer of the oxide film of mild steel [45, 48]. Another possibility is that Zn^{2+} directly makes a bond with OH^- of oxide film (oxide film contains so many OH^-) and thus form a metal cation layer on the oxide film (Fig. 13 (c)) [18, 19]. Several studies also have shown that metal cations that have large *X* can easily bond with OH^- on the oxide film of mild steel [18, 19, 28, 29]. The anodic area may be smaller than the cathodic area and the zinc layer may also cover the anodic area. Therefore, the metal cation layer of Zn^{2+} would have good protective ability against the Cl^- attack in the solution, and the protective layer would prevent the cathodic and anodic reactions (Fig. 13 (d)) on the mild steel [18, 19]. For this reason, the corrosion rate of the mild steel immersed in Zn_{sol} was lower than those in other solutions with metal cations.

5. Conclusion

The effects of metal cations on mild steel corrosion in 10 mM Cl^- aqueous solution were investigated by SEM, EDS, XPS, and EIS.

1. The corrosion behavior of mild steel in the 10 mM Cl- aqueous solution was changed with *X*, while corrosion rate was not highly correlated with *X*.
2. Different surface morphologies were observed by SEM, and it was found that some corrosion products were deposited on the surface after immersion in the Zn_{sol}.
3. Among the metal cations used in this study, only Zn^{2+} was detected by XPS on the specimen surface after immersion in the Zn_{sol}.

4. Zn^{2+} forms a protective layer with the oxide film of mild steel in the solution, and thus inhibits the electrochemical reactions, and consequently lowers the corrosion rate as well.

Acknowledgements

This study was supported by the Salt Science Research Foundation, No. 1609, XPS analysis was conducted at the Laboratory of XPS analysis, Hokkaido University, supported by 'Nanotechnology Platform' Program of the Ministry of Education, Culture, Sports, Science and Technology (MEXT), Japan, and the SEM-EDS observation of this study was conducted at the Laboratory of XPS analysis, Hokkaido University, supported by 'Material Analysis and Structure Analysis Open Unit (MASAOU)'.

References

[1] R. E. Melchers, Modelling immersion corrosion of structural steels in natural fresh and brackish waters, Corros. Sci., 48 (2006) 4174-4201.

[2] G. S. Vasyliev, The influence of flow rate on corrosion of mild steel in hot tap water, Corros. Sci., 98 (2015) 33-39.

[3] C. P. Gardiner and R. E. Melchers, Corrosion of mild steel by coal and iron ore, Corros. Sci., 44 (2002) 2665-2673.

[4] R. T. Foley, Role of the chloride ion in iron corrosion, Corrosion, 26 (1970) 58-70.

[5] H. Fang, B. Brown and S. Nesic, Effects of sodium chloride concentration on mild steel corrosion in slightly sour environments, Corrosion, 67 (2011) 1-12.

[6] T. Haruna, K. Domoto and T. Shibata, Effect of sulfate ion on corrosion of carbon steel in carbonate/bicarbonate solutions, Japan Society of Corrosion Engineering, 51 (2002) 350-355.

[7] G. C. White, Current chlorination and dechlorination practices in the treatment of potable water, wastewater and cooling water. In: Jolley RL, ed. Water chlorination: environmental impact and health effects. Ann Arbor, MI, Ann Arbor Sci., 1 (1978) 1-18.

[8] G. R. Dychdala, Chlorine and chlorine compounds. In: Black SS, ed. Disinfection, sterilization and preservation, second edition. Philadelphia, PA, Lea and Febiger, (1977) 167-195.

[9] Guidelines for drinking water quality, second edition. Health criteria and other supporting information. World Health Organization, Geneva (1996).

[10] H. J. Engell and N. D. Stolica, Untersuchungen über lochfraß an passiven elektroden aus unlegiertem Stahl in chlorionenhaltiger schwefelsäure, Arch. Eisenhuttenw, 30 (1959) 239-248.

[11] L. A. Krebs, J. Kruger, M. B. Ives, J. L. Luo, and J. R. Rodda, Passivity of metals and semiconductors, The Electrochemical Society, Pennington, NJ (2001) 561-562.

[12] D. D. Macdonald, The point defect model for the passive state, J. Electrochem. Soc., 139, (1992) 3434-3449.

[13] E. McCafferty, Introduction to corrosion science, Springer (2010) 283-286.

[14] H. J. Engell, Stability and breakdown phenomena of passivating films, Electrochim. Acta, 22 (1977) 987-993.

[15] K. G. Weil and D. Menzel, Die einwirkung von halogenionen auf passives eisen, Z. Electrochem. Soc., 63 (1959) 669-673.

[16] S. Miyake, Study on the corrosion of iron by electron diffraction, Sci. Papers Inst. Phys. Chem. Res., 36 (1939) 363-370.

[17] E. McCafferty, Sequence of steps in the pitting of aluminum by chloride ions, Corros. Sci., 45 (2003) 1421-1438.

[18] K. Otani, M. Sakairi, Effects of metal cations on corrosion of mild steel in model fresh water, Corros. Sci., 111 (2016) 302-312.

[19] K. Otani, M. S. Islam and M. Sakairi, Inhibition ability of gluconates for fresh water corrosion of mild steel enhanced by metal cations, J. Electrochem. Soci., 164 (2017) C498-C504.

[20] M. Kato, Inhibitive effect of aluminium ion for iron corrosion in water (Japanese), Boshoku Gijutsu, 31 (1982) 27-33.

[21] S. Takasaki, Development of environmentally acceptable technology for cooling water treatment, Zairyo-to-Kankyo, 64 (2015) 114-120.

[22] M. Mahdavian and R. Naderi, Corrosion inhibition of mild steel in sodium chloride solution by some zinc complexes, Corros. Sci., 53 (2011) 1194-1200.

[23] R. A. Prabhu, T. V. Venkatesha and B. M. Praveen, Electrochemical study of the corrosion behavior of zinc surface treated with a new organic chelating inhibitor, International scholarly research network, ISRN Metallurgy, (2012) 1-7.

[24] J. Xu, L. Jiang, W. Wang, L. Tang and L. Cui, Effectiveness of inhibitors in increasing chloride threshold value for steel corrosion, Water Sci. and Eng., 6 (2013) 354-363.

[25] G. N. Lewis, Valence and the structure of atoms and molecules, The Chemical Catalog Co., New York (1923).

[26] R. G. Pearson, Hard and soft acids and bases, J. Am. Chem. Soc., 85 (1963) 3533-3539.

[27] K. Otani, M. Sakairi, R. Sasaki, A. Kaneko, Y. Seki, Effect of metal cations on corrosion behavior and surface film structure of the A3003 aluminum alloy in model tap waters, J. Solid State Electrochem., 18 (2014) 325-332.

[28] M. Misono, E. Ochiai, Y. Saito, Y. Yoneda, A new dual parameter scale for the strength of lewis acids and bases with the evaluation of their softness, J. Inorg. Nucl. Chem., 29 (1967) 2658-2691.

[29] S. Zhang, T. Shibata, T. Haruna, Inhibition of metal cations to intergranular stress corrosion cracking of sensitized Type 304 stainless steel, Corros. Sci., 47 (2005) 1049-1061.

[30] K. F. Ankinpelumi, Investigation the effect of pH level on corrosion rate, University of Lagos, Lagos (2012).

[31] I. A. Ammar and S. Riad, Effect of pH on corrosion potentials, J. Phys. Chem., 62 (1958) 150-154.

[32] The chemical society of Japan, Handbook of chemistry basic, edition 2, Maruzen, Tokyo, 2004 (Japanese).

[33] J. Han, B. N. Brown, D. Young and S. Nesic, Mesh-capped probe design for direct pH measurements at an activity corroding metal surface, J. Appl. Electrochem., 40 (2010) 683-690.

[34] I. Martinez, C. Andrade, Application of EIS to cathodically protected steel: tests in sodium chloride solution and in chloride contaminated concrete, Corros. Sci., 50 (2008) 2948-2958.

[35] A. Popova, M. Christov, A. Vasilev, Inhibitive properties of quaternary ammonium bromides of N-containing heterocycles on acid mild steel corrosion. Part II: EIS results, Corros. Sci., 49 (2007) 3290-3302.

[36] D. A. Lopez, S.N. Simison and S.R. de Sanchez, Inhibitors performance in CO_2 corrosion EIS studies on the interaction between their molecular structure and steel microstructure, Corros. Sci., 47 (2005) 735-755.

[37] B. Hirschorn, M. E. Orazem, B. Tribollet, V. Vivier, I. Frateur and M. Musiani, Determination of effective capacitance and film thickness from constant-phase-element parameters, Electrochim. Acta, 55 (2010) 6218-6227.

[38] M. E. Orazem, I. Frateur, B. Tribollet, V. Vivier, S. Marcelin, Dielectric properties of materials showing constant-phase-element (CPE) impedance response. J. Electrochem. Soci., 160 (2013) C215-C225.

[39] P. C. Torres, T. J. Mesquita and R. P. Nogueira, Relationship between the origin of constant-phase element behavior in electrochemical impedance spectroscopy and electrode surface structure, J. Phys. Chem. 119 (2015) 4136-4147.

[40] G. J. Brug, A. L. G. Van Den Eeden, M. S. Rehbach and J. H. Sluyters, The analysis of electrode impedances complicated by the presence of a constant phase element, J. Electroanal Chem., 176 (1984) 275-295.

[41] I. Iitaka, S. Miyake, T. Iimori, Examination of passive iron by electron diffraction, Nature, 139 (1937) 156.

[42] M. Cohen, An electron diffraction study of films formed by sodium nitrite solution on iron, J. Phys. Chem., 56 (1952) 451-453.

[43] E. McCafferty and J. P. Wightman, Determination of the concentration of surface hydroxyl groups on metal oxide films by a quantitative XPS method, Surf. Inter. Anal., 26 (1998) 549–564.

[44] A. Valeria and M. A. Christopher Brett, Characterization of passive films formed on mild steels in bicarbonate solution by EIS, Electrochim. Acta, 47 (2002) 2081-2091.

[45] M. Pourbaix, Atlas of electrochemical equilibria in aqueous solutions, National Association of Corrosion Engineers, Huston, Texas (1974).

[46] A. Y. Chatalov, Effect du pH sur le comportement electrochimique des metaux et leur resistance a la corrosion, Dokl. Akad. Naouk S. S. S. R., 86 (1952) 7-775.

[47] E. Tada and H. Kaneko, Galvanic corrosion of a Zn/steel couple in aqueous NaCl, ISIJ Int., 51 (2011) 1882-1889.

[48] O. T. De Rincon, O. Perez, E. Paredes, Y. Caldera, C. Urdaneta and I. Sandoval, Long-term performance of ZnO as a rebar corrosion inhibitor, Cement and Concrete Composites, 24 (2002) 79-87.

Tables and Figures

Table 1 Chemical composition of specimen (mass %)

C	Si	Mn	P	S	Fe
0.020	0.010	0.180	0.015	< 0.01	Bal.

Table 2 pH of the solution used for immersion tests, initial value (pH_{int}), after adjust (pH_{adj}) and after immersion of specimens (pH_{corr}).

Test solutions	pH_{int}	pH_{adj}	pH_{corr}
Na_{sol}	5.8	5.8	6.3
Mg_{sol}	5.8	5.8	6.5
Zn_{sol}	5.8	5.8	6.5
Al_{sol}	4.2	5.7	6.5
Zr_{sol}	3.8	5.8	6.5

Table 3 The simulated values of CPE parameters of mild steel after immersion in the solutions for 1 h.

Solutions	R_{sol} ($k\Omega cm^2$)	R_{ct} ($k\Omega cm^2$)	Q ($\mu s^n \Omega^{-1} cm^{-2}$)	n
Na_{sol}	0.45	5.83	10.0	0.77
Mg_{sol}	0.43	8.81	4.93	0.77
Zn_{sol}	0.43	25.0	2.04	0.74
Al_{sol}	0.44	9.88	6.60	0.83
Zr_{sol}	0.46	11.73	8.20	0.82

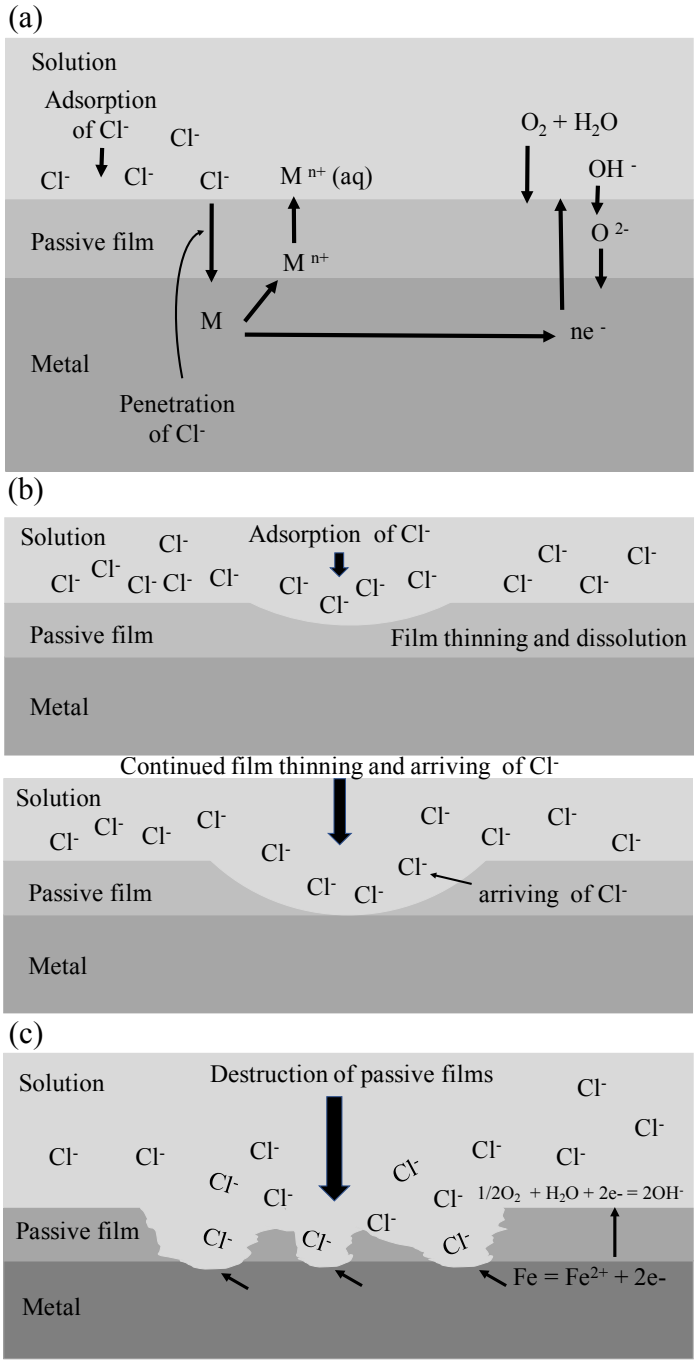


Fig. 1 Schematic representation of adsorption of Cl^- on the metal surface by (a) penetration, (b) film thinning, and (c) dissolution with electrochemical reactions on mild steel surface in 10 mM Cl^- aqueous solution.

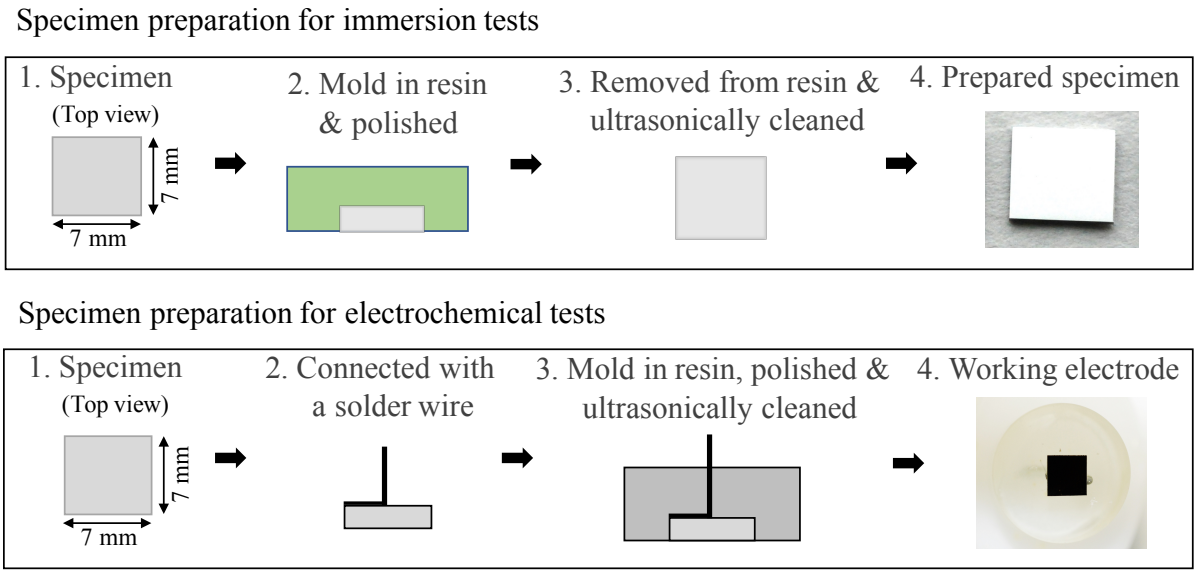


Fig. 2 Schematic images of methods used to prepare the specimens for immersion tests and electrochemical tests.

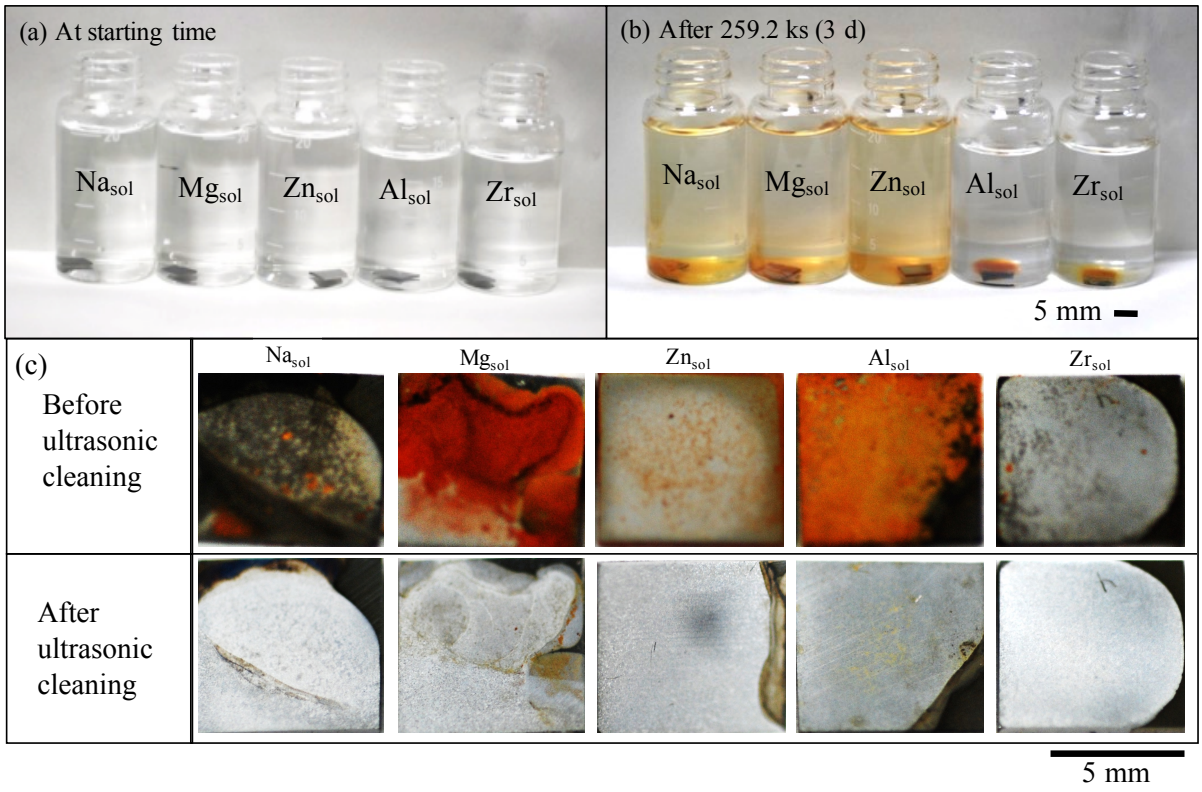


Fig. 3 Appearance of specimens after immersion in the solutions of metal cation (a) at starting time, (b) at immersion for 259.2 ks (3 d), and (c) surface images of specimens after immersion in the solutions for 259.2 ks.

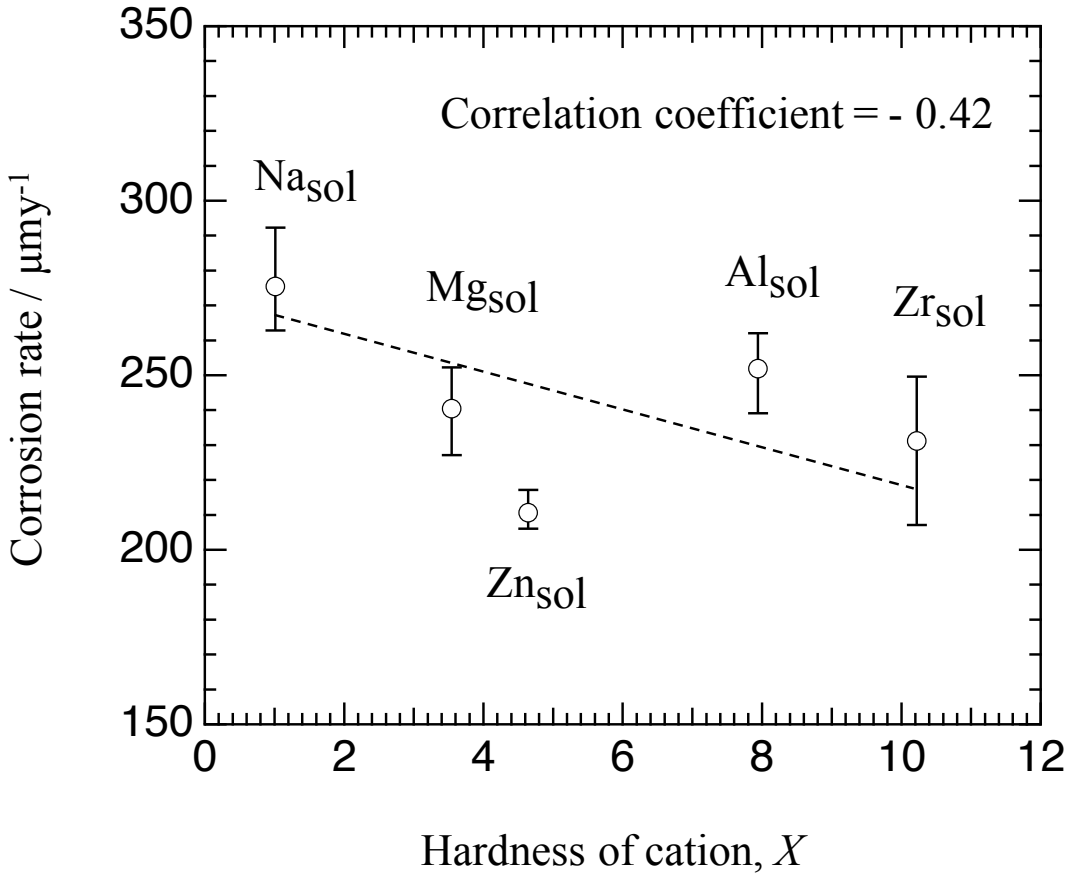


Fig. 4 Corrosion rate as a function of hardness of metal cation, X.

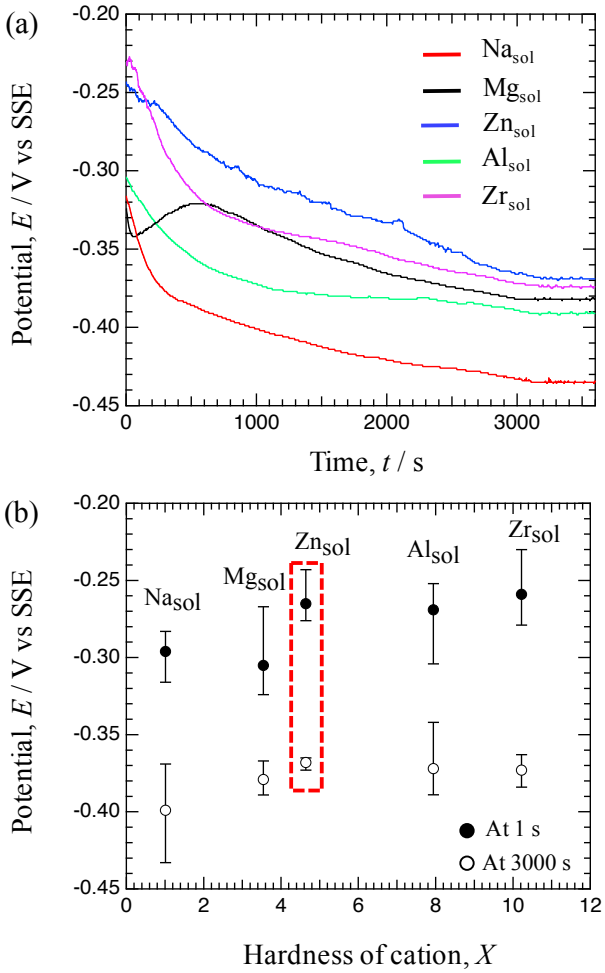


Fig. 5 (a) Open-circuit potential during the immersion tests in different solutions and (b) open-circuit potential of specimen during immersion at 1 s and at 3000 s.

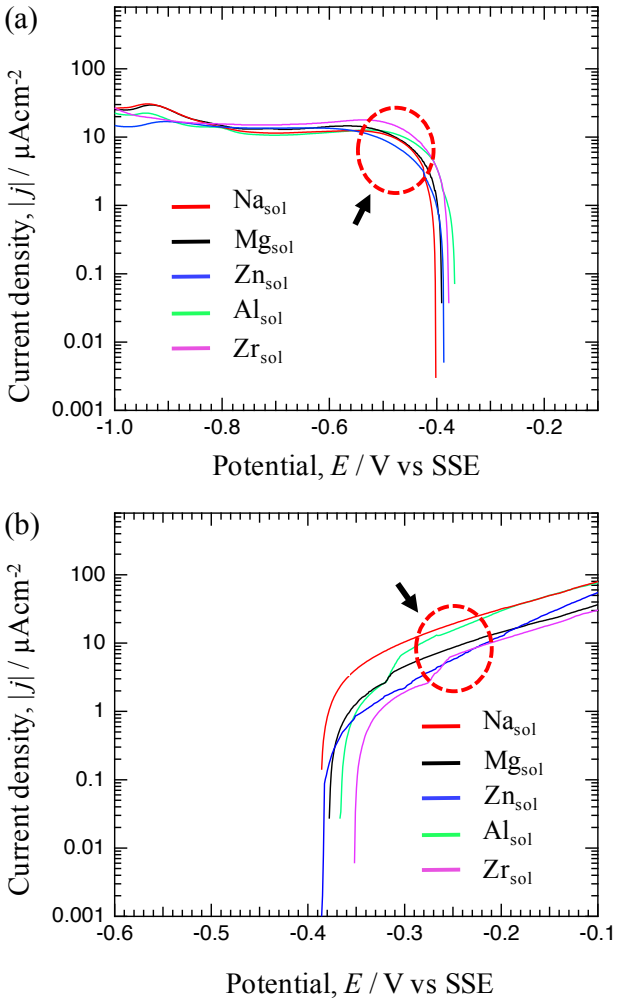


Fig. 6 (a) Cathodic and (b) anodic polarization curves of specimen immersed in the different solutions with metal cations.

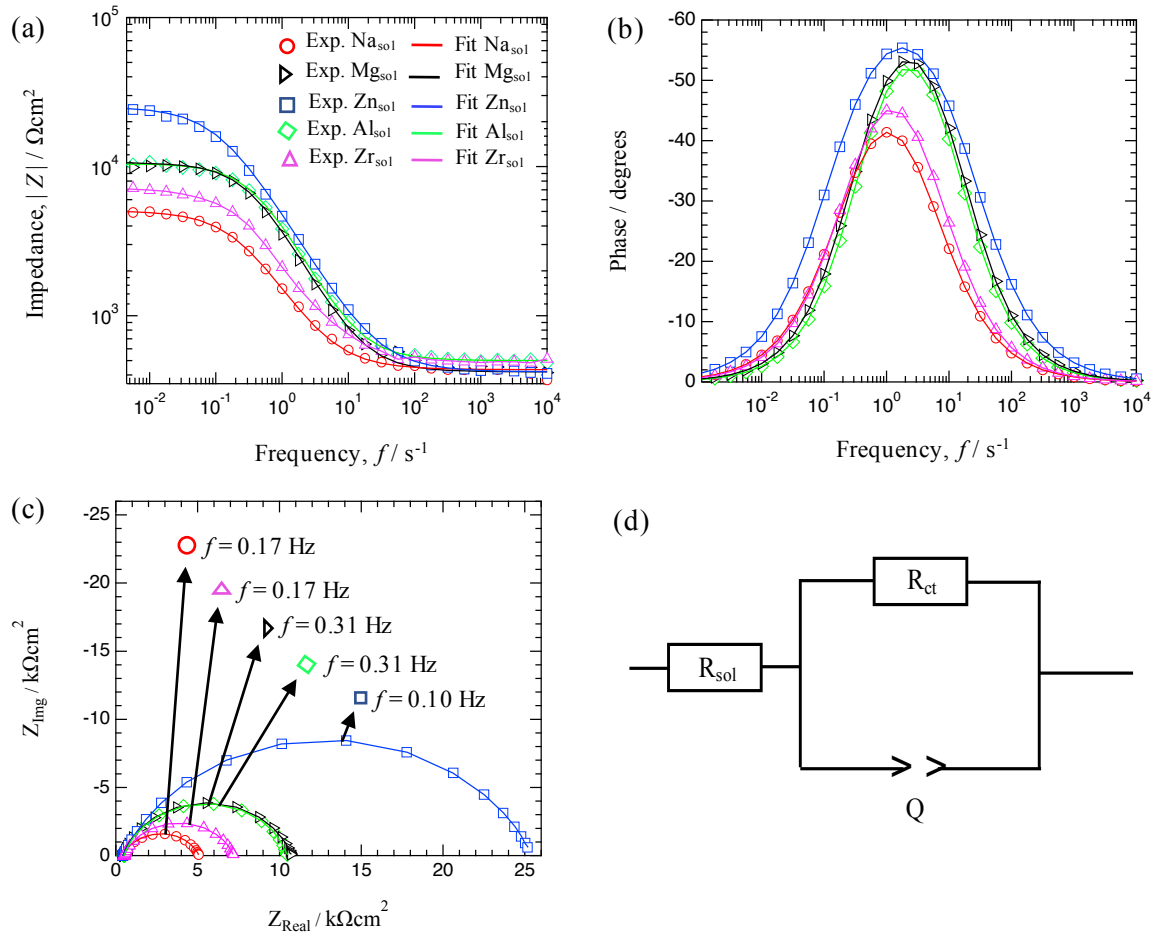


Fig. 7 Results of EIS after immersion for 1 h in the solutions with metal cations, Bode diagram of (a) Impedance and (b) phase shift plots, (c) Nyquist plots, and (d) equivalent circuit model used to fit the EIS data.

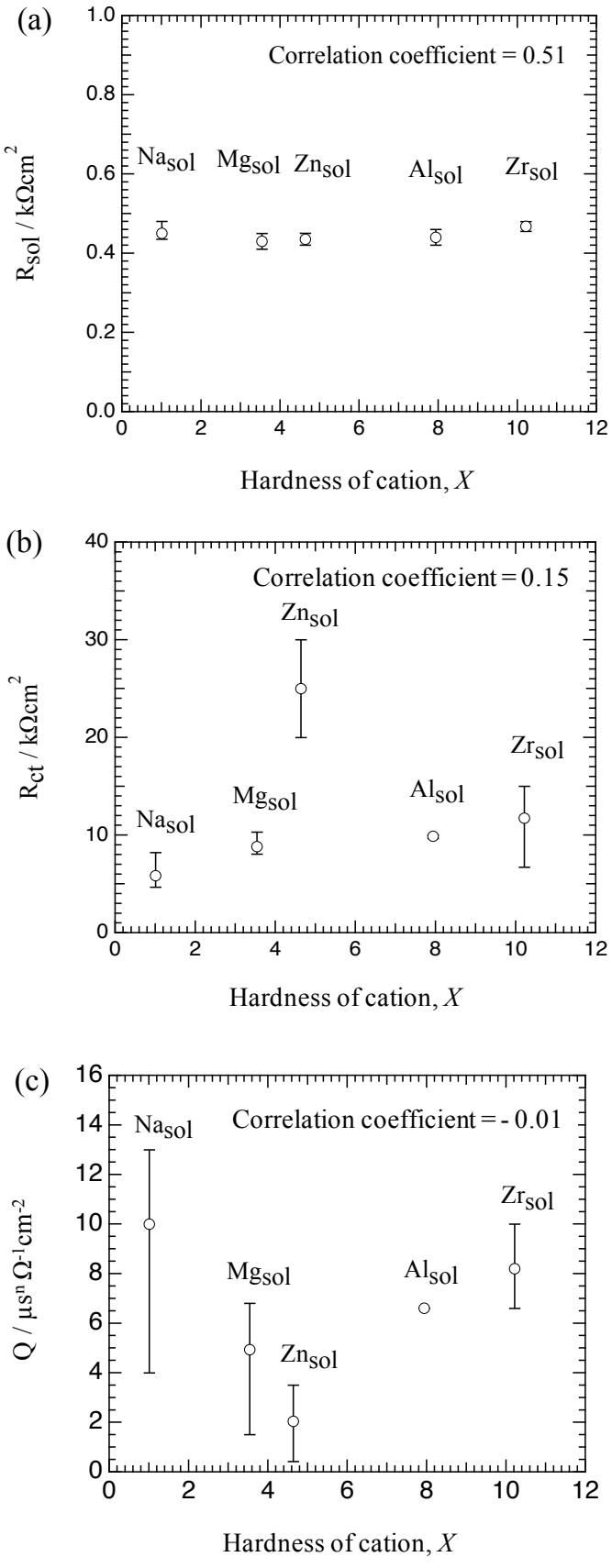


Fig. 8 Changes of (a) R_{sol}, (b) R_{ct} and (c) Q with X (hardness of metal cation).

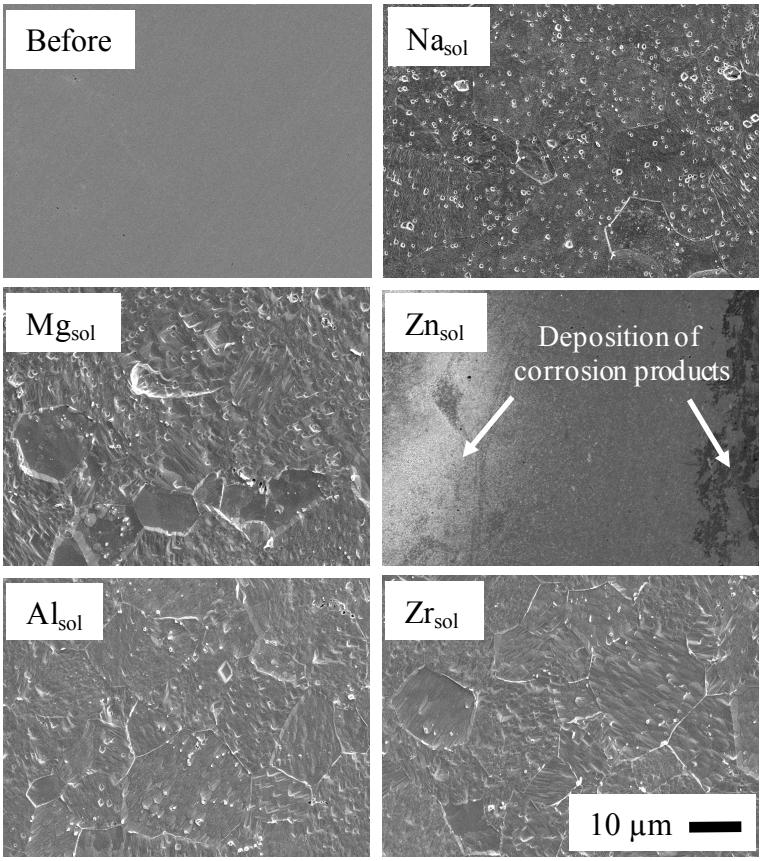


Fig. 9 Surface SEM images of specimen after immersion in the solutions for 259.2 ks at 25°C.

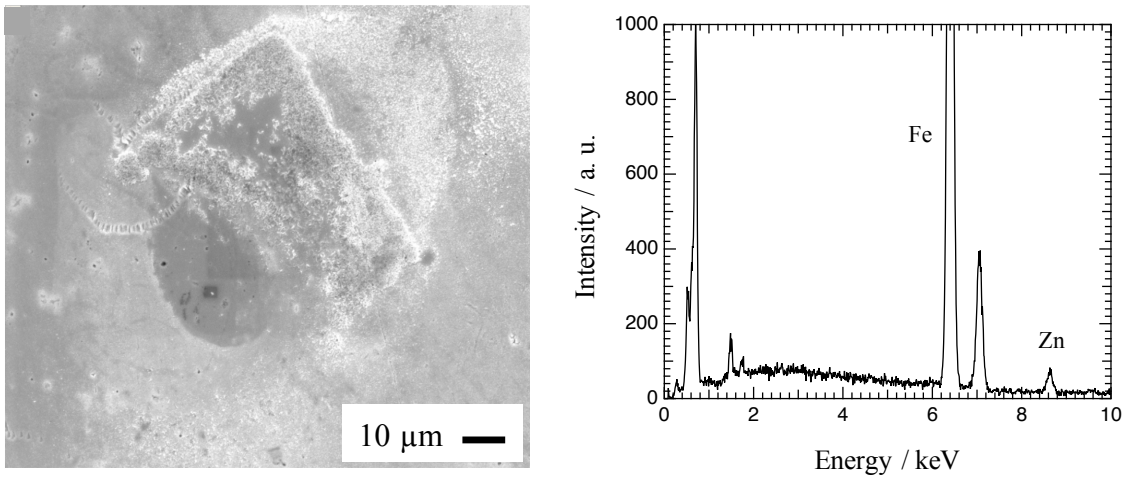


Fig. 10 SEM image of analysis area (left) and EDS results (right) of the specimen surface after immersion in the Zn_{sol}.

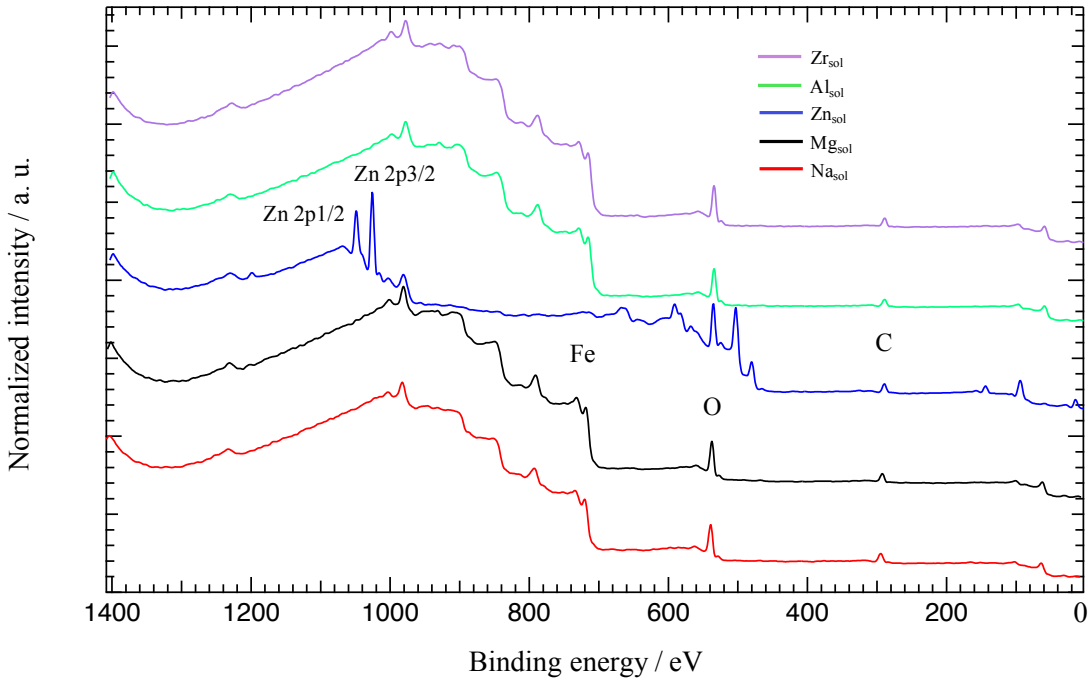


Fig. 11 XPS wide spectra of mild steel surface after immersion in the solutions with metal cations.

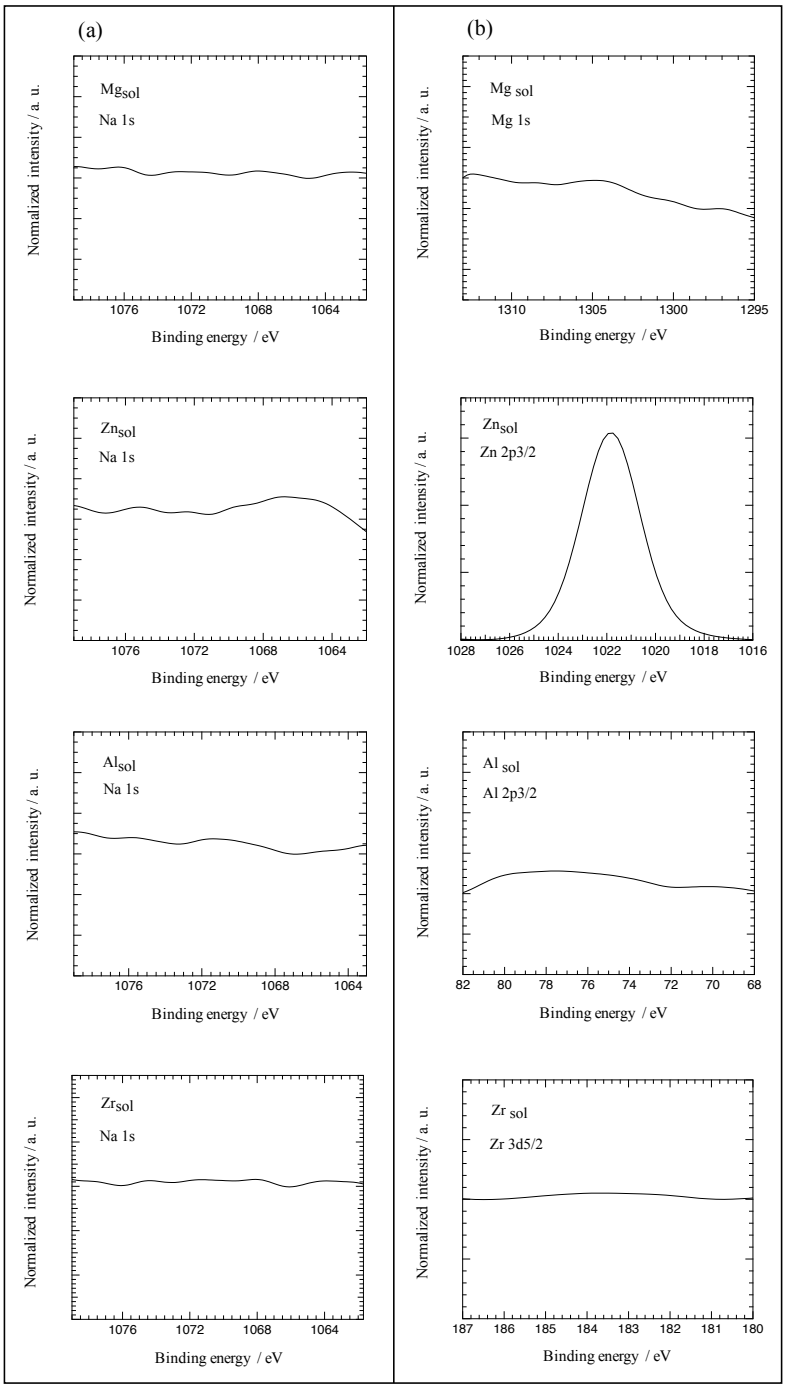


Fig. 12 XPS narrow spectra of (a) Na 1s, and (b) Mg 1s, Zn 2p3/2, Al 2p3/2 and Zr 3d5/2 after immersion in the solutions of metal cations.

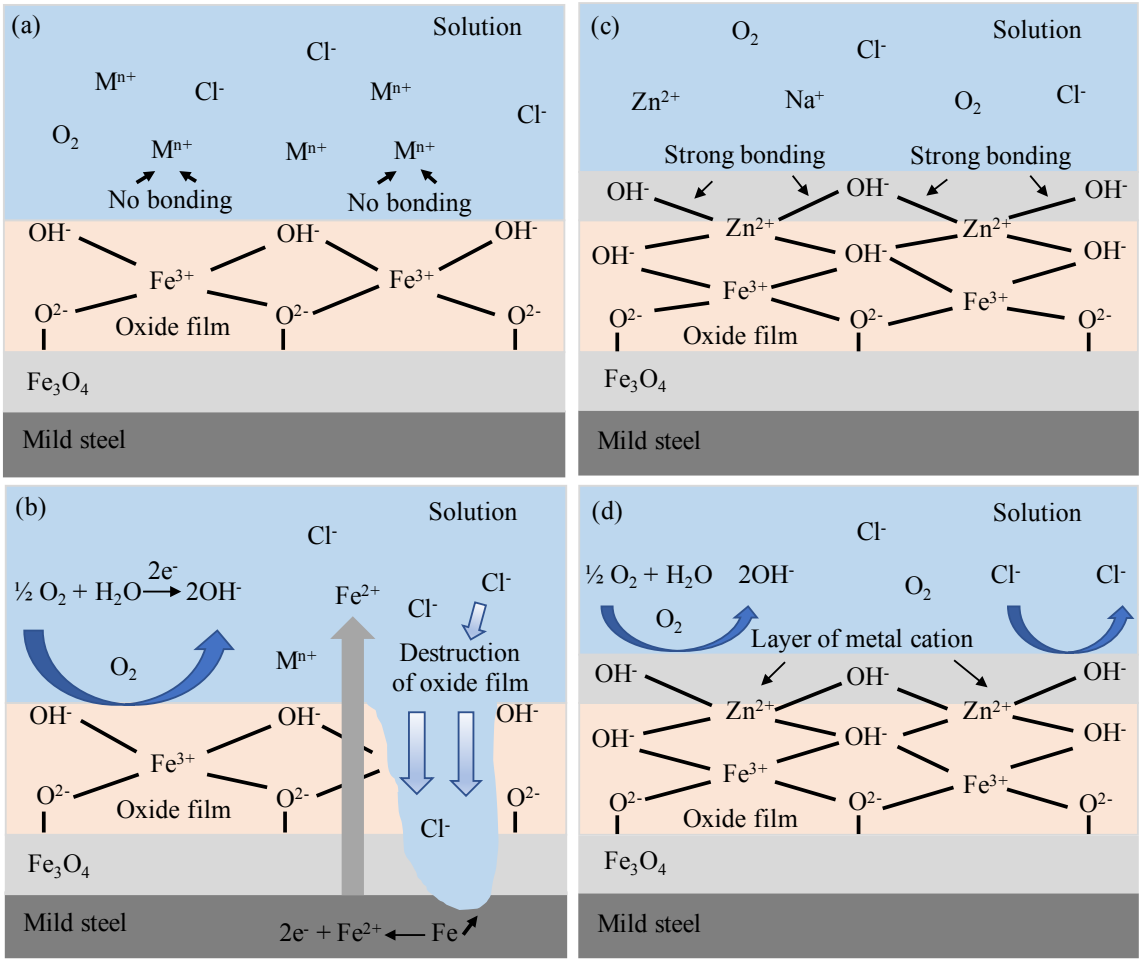


Fig. 13 (a) and (b) possible corrosion mechanism of metal cations (M^{n+} = Na^{+}, Mg^{2+}, Al^{3+}, and Zr^{4+}) with the passive film of mild steel in 10 mM Cl^{-} aqueous solution, (c) and (d) possible corrosion inhibition mechanism of Zn^{2+} with the passive film of mild steel in 10 mM Cl^{-} aqueous solution.